NAVAL POSTGRADUATE SCHOOL
MONTEREY, CALIFORNIA

THESIS

VERTICAL AND HORIZONTAL LENGTH SCALES OF SUSPENDED SEDIMENT IN THE NEARSHORE

by

Michael P. Huck

September 1998

Thesis Advisor:	E. B. Thornton
Thesis Co-Advisor:	T. P. Stanton

Approved for public release; distribution is unlimited.

REPORT DOCUMENTATION PAGE

Form Approved OMB No. 0704-0188

1. AGENCY USE ONLY *(Leave blank)*	2. REPORT DATE September 1998	3. REPORT TYPE AND DATES COVERED Master's Thesis

4. TITLE AND SUBTITLE Vertical and Horizontal Length Scales of Suspended Sediment in the Nearshore

5. FUNDING NUMBERS

6. AUTHOR(S) Michael P. Huck

7. PERFORMING ORGANIZATION NAME(S) AND ADDRESS(ES)
Naval Postgraduate School
Monterey, CA 93943-5000

8. PERFORMING ORGANIZATION REPORT NUMBER

9. SPONSORING/MONITORING AGENCY NAME(S) AND ADDRESS(ES)

10. SPONSORING/MONITORING AGENCY REPORT NUMBER

11. SUPPLEMENTARY NOTES The views expressed in this thesis are those of the author and do not reflect the official policy or position of the Department of Defense or the U.S. Government.

12a. DISTRIBUTION/AVAILABILITY STATEMENT
Approved for public release; distribution is unlimited.

12b. DISTRIBUTION CODE

13. ABSTRACT *(maximum 200 words)*

Suspended sediment measurements acquired using acoustic and optical sensors are analyzed to determine the vertical and horizontal coherence length scales in the nearshore zone across a barred beach during the SandyDuck experiment.

Suspended sediments over the vertical, from the seafloor to approximately 65 cm above the bed, are inferred from acoustical backscatter of a 1.3 Mhz signal at discrete 1.7 cm bins. The height of the bedload layer ranged from 1.7 – 3.4 cm above the bed floor for all stations investigated, which is twice the height of the theoretical wave boundary layer. The vertical coherence length was found to be an order of magnitude greater than the wave boundary layer and had a weak dependence with wave height, depth of water and orbital excursion (linear correlation coefficient of 0.6 statistically significant at 95% confidence).

The cross-shore horizontal coherence length scale of suspended sediment was determined using a two meter lagged array of six optical backscatter sensors at an elevation of approximately 18 cm above the bed. The horizontal coherence length scale was approximately 0.8 times the rms wave orbital excursion length for all cross shore stations. Both the vertical and horizontal coherence length scales are longest for infragravity waves and decrease with increasing frequency.

SUBJECT TERMS Suspended Sediment Length Scales, Suspended Sediment, Nearshore			15. NUMBER OF PAGES 58
			16. PRICE CODE
17. SECURITY CLASSIFICATION OF REPORT Unclassified	18. SECURITY CLASSIFICATION OF THIS PAGE Unclassified	19. SECURITY CLASSIFICATION OF ABSTRACT Unclassified	20. LIMITATION OF ABSTRACT UL

NSN 7540-01-280-5500 Standard Form 298
(Rev. 2-89)

Prescribed by ANSI Std. 239-18 298-102

Approved for public release; distribution is unlimited.

VERTICAL AND HORIZONTAL LENGTH SCALES OF SUSPENDED SEDIMENT IN THE NEARSHORE

Michael Patrick Huck
Lieutenant, United States Navy
B.S., United States Naval Academy, 1990

Submitted in partial fulfillment
of the requirements for the degree of

MASTER OF SCIENCE IN PHYSICAL OCEANOGRAPHY

from the

NAVAL POSTGRADUATE SCHOOL
September 1998

ABSTRACT

Suspended sediment measurements acquired using acoustic and optical sensors are analyzed to determine the vertical and horizontal coherence length scales in the nearshore zone across a barred beach during the SandyDuck experiment.

Suspended sediments over the vertical, from the seafloor to approximately 65 cm above the bed, are inferred from acoustical backscatter of a 1.3 Mhz signal at discrete 1.7 cm bins. The height of the bedload layer ranged from 1.7 – 3.4 cm above the bed floor for all stations investigated, which is twice the height of the theoretical wave boundary layer. The vertical coherence length was found to be an order of magnitude greater than the wave boundary layer and had a weak dependence with wave height, depth of water and orbital excursion (linear correlation coefficient of 0.6 statistically significant at 95% confidence).

The cross-shore horizontal coherence length scale of suspended sediment was determined using a two meter lagged array of six optical backscatter sensors at an elevation of approximately 18 cm above the bed. The horizontal coherence length scale was approximately 0.8 times the rms wave orbital excursion length for all cross shore stations. Both the vertical and horizontal coherence length scales are longest for infragravity waves and decrease with increasing frequency.

TABLE OF CONTENTS

I. INTRODUCTION.....1

II. EXPERIMENT.....5

III. RESULTS.....9

A. DATA ANALYSIS.....9

B. VERTICAL SPATIAL COHERENCE OF SEDIMENT.....12

C. HORIZONTAL SPATIAL COHERENCE OF SEDIMENT.....16

IV. DISCUSSION.....19

A. HORIZONTAL SCALE.....19

B. BEDLOAD LAYER HEIGHT.....21

C. VERTICAL COHERENCE.....22

V. SUMMARY AND CONCLUSIONS.....25

LIST OF REFERENCES.....27

INITIAL DISTRIBUTION LIST.....45

I. INTRODUCTION

Sand transport on beaches is generally divided into bedload and suspended load. Transport as suspended load is thought by some to be the primary mode of transport and is therefore very important to erosion and accretion. However, the mechanisms that drive sediment suspension are poorly understood. Previous studies of suspension of sediment in the nearshore environment have investigated a range of wave frequencies and a number of possible mechanisms.

Considerable insight into suspended sediment processes has been obtained from field measurements using vertical arrays of optical backscatter sensors (OBS) and acoustic backscatter profilers. Observations in the nearshore show suspended sediment transport is dependent on height above the bed, wave type and distance from the breakpoint. Using OBS sensors, Beach and Sternberg (1996) found that plunging waves are responsible for a greater proportion of the suspended load than bores, spilling waves and unbroken waves. Yu et al. (1993) found that suspended sediment concentrations occurred within the wave boundary layer for unbroken waves. Nearbed concentrations increased as waves approached the breakpoint. Under breaking waves, suspended sediment concentrations increased dramatically, and sediment inversions and localized high concentration patches of sediment were present.

Beach and Sternberg (1987) found that strong low frequency (<0.01Hz) fluid motions accounted for over 85% of the total spectral energy. Sediment suspension events associated with infragravity waves persisted for periods of 30 – 45 seconds occurring at elevations of at least 26 cm and were 5 times greater near the bed and 3 times greater at 50 cm than those associated with incident wave motions alone. Suspended sediment

events associated with incident waves rarely reached above 8 cm. Hanes (1991) found that there was a significant correlation between near-bed concentration and cross-shore fluid speed squared over a range of time scales, and that suspended sediment concentration was enhanced at time scales corresponding to groups of waves.

Using acoustic backscatter, Hay and Bowen (1994) found that the horizontal and vertical length scale of suspended sediment eddies was O(30cm) which was many times greater than the logarithmic wave boundary layer thickness. They attributed the origin of the sediment clouds to be vortex shedding from megaripples, enhanced by the interaction of the largest wave in the group with the bottom.

Sediment eddy diffusivities in the nearshore have been studied by acoustic backscatter (Sheng and Hay, 1995). Water depth was used as used as a height scale for vertical profiles of sediment eddy diffusivity. Comparisons indicated that the height scale was significantly less than total water depth, and that a single, constant, height scale did not collapse the data to a single curve. It was suggested that multiple vertical length scales, which would include the bedform scales and combined wave-current flow, would be more appropriate.

The complex nature of the nearshore regime, including grain size, bedforms, turbulence, waves and currents, spatial and temporal variability, etc., has made it difficult to link the suspension and transport of sediment to a general physical theory. This paper investigates, through spectral analysis, the vertical and horizontal length scales of suspended sediment for a wide range of frequencies and possible mechanisms for sediment suspension in the nearshore.

The first section describes the field experiment and measurements, and discusses the criteria used to evaluate data quality. The vertical suspended sediment length scales are investigated by intercomparing the spectral coherence of suspended sediment concentrations over a profile inferred from acoustical backscatter profiles. The horizontal suspended sediment length scales are determined using the spectral coherence between optical backscatter (OBS) sensors in an array.

Several approaches are used to investigate the mechanisms that determine the vertical and horizontal suspended sediment length scales. Orbital excursion, calculated from measured cross-shore velocity, is compared with the horizontal suspended sediment length scales. Orbital excursion, wave height and depth of water are used to compare the vertical suspended sediment length scales.

II. EXPERIMENT

Sediment concentration measurements were obtained as part of the Sandy Duck experiment conducted at the U.S. Army Corps of Engineers Field Research Facility (FRF), Duck, North Carolina. The analysis is based on three days of data selected from the September - October 1997 phase of the experiment.

The beach during the experiment generally consisted of a two-bar system with a dynamic inner bar , 0-75 m offshore, and a secondary bar with lower amplitude, 195-210 m offshore (Figure 1). The mean foreshore slope of the beach was ~0.08 (1:12), and the slope offshore of the bars was ~0.011 (1:90). The tidal range was nominally 1 m for the days investigated. Sediments within the surf zone were well sorted with a mean grain size of 0.2 mm. Sediments on the foreshore were poorly sorted with larger mean grain size (>0.4 mm).

The weather during the initial measurements, September 24- October 15, was characterized by weak winds offshore and moderate wave heights, 0.4-1.5 m. From October 16-23, a storm produced predominant winds onshore, and large wave heights, 1.6 - 4.0 m. For the remainder of the month, the weather was characterized by highly variable weak winds onshore and offshore and lower wave heights of 0.5-1.5 m.

The measurements described here were taken by an acoustic backscatter profiler, a six element array of OBS sensors, a two-component electromagnetic current meter and a pressure meter. These sensors were mounted on a 3m by 5m aluminum sled constructed of 20 cm diameter pipe runners with 15 cm pipe cross members. For stability, 180 kg of lead weights plus ~450 kg of sand were placed inside the runners of this low-profile

structure. To ensure that the sled did not move while on station, four fins (45 cm wide) extending 60 cm into the sand were installed.

Each morning the sled was towed to the farthest offshore location for the first run (~175 m from the shoreline) by the 11 m high, motorized, three-wheel CRAB. A four-wheel drive forklift pulled the sled shoreward 10-30 m for subsequent measurement runs that are referred to in the text by sequential numbers (Figure 1). The length of data collection at each station was nominally 1 hour. The data were acquired during daylight and early night.

Data from the sled were transmitted to shore via a fiber-optic cable, where signals were monitored and recorded. Short cables from the sensors to the data acquisition system on the sled (<7m) resulted in low noise signals. An armored cable, married to the sled chain tether, provided power and controller signals for the instruments via two conductors and returned the digitized signals via a fiber-optic line.

The vertical profile of suspended sediments near the seabed was inferred from the acoustic backscatter signal of the Bistatic Coherent Doppler Velocity Profiler (BCDV), mounted 1.5 m from the sled on a movable cantilever arm (Figure 2). The BCDV measures backscatter from a 1.3 Mhz transducer mounted in the center of the instrument oriented approximately 90 cm from the bedfloor. A series of 1.7 cm length acoustic pulses are transmitted at a rate of 500 Hz, and the complex backscatter amplitudes are sampled every 1.7 cm, from the bed to an elevation of ~65 cm with an 80 dB dynamic range. The acoustic return measures sediment to a maximum concentration of approximately 28 g/l, before the signals are clipped.

Contained within the BCDV is a two-axis tilt sensor, with 0.1° accuracy, which enables the doppler velocity data to be transformed into an earth referenced coordinate system. By using the tilt sensors and the BCDV acoustical return of the bottom to estimate range from the bed to the transducer, the locations of the other sensors mounted on the sled were converted from a sled referenced to an earth-referenced coordinate system assuming a locally flat bed.

The OBS sensors (Seapoint turbidity meter) measure turbidity by detecting scattered light from suspended particles in the water. The optical design of the sensor restricts the angle of emission of the light source and the angle of detection of the light confining the volume of particles measured to within 5 cm of the sensor window. The sensor gain was 20x for a sensitivity of 40 mV/FTU and a range of 125 FTU (Formazin Turbidity Units) with an error of 2% up to the maximum concentration of approximately 6.1 g/l.

The six OBS sensors were aligned in the cross-shore and mounted on the moveable cantilever arm that located the sensors at a nominal elevation of 22-24 cm from the bed (Figure 2). The sensors looked downward so that they measured sediment concentrations 17-19 cm above the bed. The relative spacing of the OBS sensors were 70, 20, 10, 40, 60 cm centered on the BCDV.

Waves and mean water level were measured near the cantilever arm by a pressure sensor approximately 50 cm from the seabed (Figure 2).

The morphology of the bottom was measured at various scales. The large-scale morphology (bathymetry) was surveyed daily by the CRAB using DGPS as it traversed a grid of 20 lines covering a 700 m alongshore by 350 m cross-shore area. Contour plots of

the bathymetry show the alongshore contours from the top of the inner bar seaward to be essentially straight and parallel. Bathymetry inside the inner bar tended to be highly variable. Small-scale morphology, including ripples and megaripples, were measured relative to the CRAB by seven, 1 MHz sonic altimeters mounted on the CRAB nominally 70 cm from the bed. The altimeters have a 3.4° beam width which result in a ~4cm footprint. The returns were sampled at a rate of 48 Hz, which resulted in a sample spacing of 2-4 cm (dependent on CRAB speed) with millimeter vertical resolution and accuracy <2 cm (Gallagher et al., 1996). Bed dilation, suspended sediments in the water column and bubbles associated with breaking waves change the reflective surface, leading to decreased accuracy relative to resolution. In addition, a scanning x-y altimeter mapped the seabed directly below the sensor in a 1m longshore by 3 m cross-shore matrix to measure small-scale variation in bottom morphology. The BCDV also measured the elevation of the bed, with a 2 cm diameter footprint.

The sled orientation was determined using a digital compass mounted on the sled with an accuracy of O(1°). Two-component, horizontal velocity measurements were reduced to a shore normal right-handed coordinate system (positive offshore and to the south) by using compass data and adding at each sled position any deviation of the contour line from a shore parallel direction as determined from the CRAB measurements. Errors associated with the rotation of the coordinate system are comparable to the velocity offsets errors, and therefore are ignored.

Meteorological information of wind, air temperature, atmospheric pressure, and sea surface temperature were recorded simultaneously at the seaward end of the 600 m long FRF pier and atop the FRF building in front of the pier.

III. RESULTS

A. DATA ANALYSIS

The objective of the analysis is to use robust spectral techniques, which require relatively long time series of high quality data. Data selected for analysis were screened based on instrumentation limitations. The OBS sensors were limited by too high a gain selection and inability to discriminate fines and high concentrations of bubbles from sediments. The gain selected for turbidity sensors limited the maximum sediment concentrations to 6.1 g/l, which often was too low. This resulted in clipping of the signals, which artificially increased coherence between sensors. The increased wind and wave heights associated with the storm event, after October 15, resulted in suspended sediment concentration exceeding 6.1 g/l and therefore, these data were not used.

At times during the experiment large amounts of fines (mud size particles) discharged from the Chesapeake Bay were present in the water column. The optical backscatter intensity by fines at the times of highest intrusion of muddy water was equal to or greater than that of suspended sediments. The purpose of this paper deals with the investigation of suspended sediment from the bed floor, not the movement of fines within the water column. Even after the time series were demeaned and detrended, the fines resulted in low frequency signals with oscillations of 10 min – 1 hour. These events caused the coherence between sensors to be high at low frequencies, resulting in an artificially high coherence length scale. These days were eliminated from consideration. Three days were selected to be examined in detail (see Figure 1 and Table 1).

	September 28	September 29	October 13
H_s	1.06 m	0.39 m	0.74 m
T_{peak}	6.6 sec	8.2 sec	10.7 sec
θ_{peak}	10.0 deg	-38.0 deg	2.0 deg

Table 1. The significant wave height, peak period, and peak angle measured at 8 m for the three days examined.

The suspended sediments can be acoustically distinguished from the fines by selecting the BCDV operating frequency to have the highest response to particles with mean grain size characteristic of the sediments found within the surf zone during the experiment (0.2 mm). Sensitivity and calibration is accomplished by determining the backscatter levels and attenuation for known concentrations of sand samples (Stanton and Kohanowich, 1998). The 1.3 MHz backscatter response varies with mean particle size with the fines having a much lower response than the mean grain size of Duck sand; while having an acoustic response insensitive to small deviations from the 0.2 mm grain size.

It is also difficult to discriminate bubbles from sediments in the acoustic backscatter measurements. High concentrations of bubbles occurred on higher wave days and often locally under breaking waves, further limiting available data. To address the problem of bubble discrimination, the log mean concentration profile of acoustic backscatter was examined to determine when bubble intrusion was prevalent. Since the source of sand is at the bed, sediment concentration is likely to decrease as height above the bedfloor is increased (Figure 3a). However, if large amounts of bubbles are present, the acoustic return from the bed to the BCDV will decrease to a local minimum due to the decrease in suspended sediment with height, and then increase owing to bubbles being

injected from above. When the gradient of the log mean backscatter increased by more than 1.5% for more than five bins, it was assumed that significant bubble levels were present (Figure 3b).

When a station was identified as being contaminated by bubbles in the upper water column, that station was excluded for further analysis since the presence of bubbles increased the vertical coherence and did not give a true representation of the suspended sediment concentrations. The stations excluded from the survey for the days considered due to the presence of bubbles in the water column, stations 5-9 on 28 September and stations 5-7 on 13 October, are on higher energy wave days, located shoreward of the foreshore bar, and where wave breaking occurred.

It is necessary to differentiate the seafloor in the backscatter signal from the bed and suspended load transport. The seafloor is defined as the maximum concentration return. The seafloor changed relative to the BCDV elevation as the sled settled into the seabed and had to be taken into account when assigning discrete elevation bins above the seafloor for cross-spectral analysis. Settling of the sled ranged from 0 – 28 cm while on station. Settling of the sled was corrected by taking one minute averages of the maximum return and assigning the seafloor to that bin. Subsequent bins in the water column were reordered accordingly such that the bottom is the first bin for each one-minute time interval. The stations that had to be removed from the survey due to excessive sinking of the sled are station 8 and 9 on 28 September and stations 5 and 6 on 29 September. Excessive sinking is defined when the elevation changed more than 20 cm in the one hour. Stations 8 and 9 on September 28 are the stations closest to the shoreline, and also were excluded because of significant bubble contamination associated with wave

breaking.

After considering the various data criteria, ten stations are analyzed in detail for the three days, which are indicated by circled station numbers in Figure 1. Examples of suspended sediment time series and spectra for 28 September are shown in Figure 4. The time series illustrates the episodic nature of suspended sediments and the background variations due to sea-swell waves. The spectra show that suspended sediment variation is most significant at the infragravity wave band.

Spectra of cross-shore velocity for each day at station 4 are shown in Figure 5. The waves on these three days are associated with moderate, relatively narrow-banded, swell waves. The sediment concentration spectra above of the infragravity frequency band have similar characteristics to the cross-shore velocity spectra. To investigate the frequency dependence of suspended sediments to cross-shore velocity and wave motion, the frequency spectra was divided into four equal frequency bands, 0.0 – 0.05 Hz, 0.05 – 0.10 Hz, 0.10 – 0.15 Hz and 0.15 – 0.20 Hz. The 0.05 bandwidth was chosen to separate the infragravity waves from the sea-swell waves.

B. VERTICAL SPATIAL COHERENCE OF SEDIMENT

The vertical coherence of suspended sediments is inferred from the acoustic backscatter of the BCDV. Bedload and suspended load transport are differentiated and the vertical coherent length scale is determined by calculating the coherence between bins over the vertical. The time series near the seafloor are significantly different than those higher in the water column, with the sediment concentration near the bed an order of magnitude greater than the return higher in the water column. The contrast in acoustic

return signals is used to differentiate between bedload and suspended load. It is hypothesized that the bedload is not statistically coherent with the suspended sediment layer above it, since the bedload is the part of the total load which is supported by intergranular forces, while the suspended load is supported by fluid drag (Bagnold, 1956).

The height of the bedload layer is determined by examining the coherence between adjacent elevation bins. The bedload layer is defined as the highest bin near the bed that is incoherent, not significantly different from zero at the 95% confidence level, with the bin immediately above. Measurements on September 28 at station 1 are a good illustration of the criteria used for bedload layer determination (Figure 6). At this station the height of the bedload layer is determined to be 1.7 cm above the bed (bin 36), keeping in mind that 1.7 cm is the range resolution of the BCDV. At this level the coherency quickly goes to zero and bin 36 is incoherent with bin 35, which is at 3.4 cm above the bed. The height of the bedload layer ranged from 1.7 – 3.4 cm above the bed floor for all stations investigated.

The vertical coherence length scale of suspended sediment is calculated by intercomparing the coherence between the reference bin to all bins above it; then determining the distance from the bed to the level at which coherence is no longer significantly different from zero at the 95% confidence level (with 160 degrees of freedom in this case). The nominally one hour time series are divided into 16 samples giving 32 degrees of freedom at the 0.009 Hz resolution for the spectra. The spectra and cross-spectra were then averaged over the 0.05 Hz bands, increasing the degrees of freedom. The reference level is defined as the level nearest the seafloor which is incoherent with the bedload layer, gave the largest vertical coherence with the bins above

it, and had the smallest variation between frequency bands. The coherence analysis for 29 September at station 2 is an example of the criteria used (Figure 7). At 1.7 cm from the bed, bin 37, the sediment concentration and coherence with all other bins is consistent with the bedload layer (Figure 7a). At 3.4 cm above the bed, bin 36 (Figure 7b), the coherence length scale increases, but the coherence length is not consistent until comparison with bin 34, 6.9 cm from the bed (Figure 7c). The reference elevation of 8.6 cm, bin 33, was chosen because it is the lowest bin at which the largest vertical length scale is achieved and the variability in frequency bands is minimized (Figure 7d). If the reference level was raised, for example to 10.3 cm, bin 32, there would be no gain in coherence length scale or decreases in frequency variability. The reference level ranged from 5.1 – 9.4 cm above the bed for all the stations examined. For most stations using these criteria there was a difference between the defined bedload layer and the reference level, which implies a transition region between bedload and suspended load transport.

There is a coherence spike for all frequency bands at approximately 60 cm at station 2 on 29 September, which is attributed to reverberation of the monostatic pulse train of the BCDV under low backscatter conditions(Figure 7). The coherence spike is an inherent problem in a pulse coherent system, especially in a low energy station such as station 2. The problem occurs when successive pulses reverberate off the seafloor and then reflect back from the BCDV sensor head, generating a weak range alias of energy scattered at the bed.

An example of the suspended sediment frequency spectra over the vertical is shown in Figure 8. The bottom is identified as the highest concentration (bin 38) and has a broad spectrum. The bedload transport spectra (bins 36 and 37) are similarly broad.

The reference bin spectrum (35) (denoting the elevation at which suspended sediments start) and the spectra above have considerable structure, reflecting the dominant forcing at infragravity and swell frequency waves. These spectra difference support the hypothesis of differences in the suspension mechanism in these layers

The vertical coherence length is found to be an order of magnitude greater than the wave boundary layer, and dependent on the location from the shore and the frequency band over which the coherence is determined. The dependence of vertical coherence with cross-shore position is found related to bottom morphology, H_{rms} and percentage of wave breaking. The farthest offshore stations investigated, station 1 and station 2 for 28 and 29 September, respectively, had very distinct suspended sediment layers (Figure 9). The elevation of the suspended sediment layer is consistent across all four frequency bands at both offshore locations. The coherence reduces to zero above the suspended sediment layer indicating that these sediment concentrations were below the noise threshold of the BCDV ($<10^{-3}$ g/l). The morphology measured by the sonic altimeters mounted on the CRAB at these stations is characterized by a smooth bottom (rms roughness < 1 cm).

At the next closest stations towards the shore, station 2 and station 3 for 28 and 29 September, there is a transition from the offshore stations and the stations closer to shore. The bottom changes from a flat bed to a bedfloor with a shallow incline (0.007 slope) with ripples O(2 cm) present. The variability in coherence levels between frequency bands is increased (Figure 10a), and the distinct height delineation of the suspended sediment is reduced (Figure 10b).

At stations 3 and 4 for 28 September, station 4 for 29 September, and station 3 for 13 October, waves are beginning to break and there is an increase in H_{rms}. The bottom

morphology at these stations was characterized by small ripples O(1 cm) with O(1 m) wave length present on an inclined bed (0.01 slope). At these locations there is a slower decrease in coherence with height above the bed for all four frequency bands (Figure 11). Variability in coherence between frequency bands is also increased, with forcing by infragravity waves (0.0 - 0.05 Hz) giving the highest coherence values.

The only station included well inside the surf zone is station 8 on 29 September. This station is located within the trough of the barred beach after the intense breaking on the bar. Interestingly, the data at high tide was similar to transition stations described in Figure 10. The suspended sediment coherence slowly decreased to a coherence level of 0.3 at 22 cm and remained at that level through the remainder of the observed water column, 65 cm. This suggests that there were two layers of sediment in the water column, with a high concentration of suspended sediment from the seafloor to approximately 20 cm, and a low concentration cloud of sediment (or possibly bubbles) higher in the water column.

C. HORIZONTAL SPATIAL COHERENCE OF SEDIMENT

The vertical coherence length scale at each station was calculated first to determine if the OBS sensors were within the suspended sediment layer. Since the OBS sensors observed sediment concentration at approximately 17 – 19 cm from the bedfloor, a minimum vertical coherence length scale criteria for use of the data of 20 cm is used. The stations excluded because the vertical coherence length scale is less then 20 cm are stations 1 on 20 September and stations 1 and 2 on 13 October. The excluded stations

were located farthest offshore where the depths are the greatest, there is no wave breaking, and wave heights for the day were moderate to low.

In calculating the horizontal coherence, the turbidity data were first decimated down from 48 to 2 Hz, resulting in a Nyquist frequency of 1 Hz. The one-hour data records were then divided into 16 sample functions and detrended to minimize the effects of fines. The coherence for various frequency bands was calculated for each combination of OBS channels and plotted against the spatial distance between sensors.

The horizontal coherence length scale is found dependent upon the frequency band, wave height and orbital excursion (see Figure 12 as an example). A horizontal coherence length scale is defined as the e-folding scale determined by fitting an exponential least square curve to the coherence as a function of distance. The greatest values of the horizontal length scale are associated with infragravity waves (0.0 – 0.05 Hz). The peak wave frequency has the next highest coherence length scale.

The horizontal length scale and variability between frequencies is proportional to the wave height. As the wave height increases, the horizontal length scale and frequency variability increase. On the low wave height day of September 29, the horizontal length scales were less and the deviation of the length scale between stations was small compared to the larger wave height day of 28 September (Figure 12).

IV. DISCUSSION

This study of vertical and horizontal length scales was limited to three days when fines did not intrude from Chesapeake Bay and to moderate to low waves when the dominant disturbing force did not result in high suspended sediment concentrations causing clipping of the OBS signals. The stations in the horizontal were further limited because of either high bubble concentrations at the inshore stations or low vertical coherence at the farthest offshore stations. Therefore, the study was limited to cases of moderate waves outside the region of strong wave breaking.

A. HORIZONTAL SCALE

The orbital excursion at the bed averaged over each frequency band is used to scale the horizontal length scale. The rms horizontal orbital excursion for the frequency band, f_u to f_l, is

$$\xi = 2\left(\int_{f_l}^{f_u} G_\xi(f)df\right)^{1/2} \qquad (1)$$

The orbital excursion spectrum was calculated by applying the spectral integrator transfer function, $|H(f)|^2 = \omega^{-2}$, to the cross-shore velocity spectrum, $G_\xi(f) = |H(f)|^2 G_u(f)$, where the transfer function acts as a low pass filter.

The horizontal spatial coherence as a function of horizontal separation of the OBS sensors normalized by the orbital excursion is shown in Figure 13. The use of orbital excursion reduces both station variability (which is a function of H_{rms}, cross-shore velocity, and depth of water) and frequency dependence. The orbital excursion is a representative measure of the horizontal length scale of suspended sediments because it is

dependent on the velocity near the bed and on the frequency band of interest. The orbital excursion varied considerably across frequency bands due to the variability of the wave band variance, frequency and depth of water for different days and stations. For example at station 4 on September 28, when the peak frequency is in the 0.10 – 0.15 Hz frequency band, the orbital excursion for each frequency band is 2.53 m (0.0 – 0.05 Hz), 0.46 m (0.05 – 0.10 Hz), 0.83 m (0.10 – 0.15 Hz), 0.46 m(0.15 – 0.20 Hz). On October 13, the peak frequency is in the swell band, 0.05 – 0.10 Hz, and the second highest coherence length scale is in that band. The range of orbital excursion values for various bands are summarized in Table 2.

Frequency Band	Range of Values for Orbital Excursion	Mean/ Standard Deviation for Orbital Excursion	Mean Horizontal Coherence/Orbital Excursion
0.0 – 0.05 Hz	0.71 – 2.53 m	1.51/0.61 m	0.67
0.05 – 0.10 Hz	0.27 – 0.85 m	0.45/0.20 m	0.92
0.10 – 0.15 Hz	0.37 – 0.86 m	0.60/0.20 m	0.83
0.15 – 0.20 Hz	0.12 – 0.46 m	0.29/0.15 m	1.78

Table 2. The range, mean and standard deviation of the orbit excursion for all frequency bands. The mean value for all frequency bands of the horizontal coherence length scaled by orbital excursion.

A mean horizontal coherence length scaled by the orbital excursion is calculated as the e-folding length by fitting a least square exponential curve to the data (Figure 13). The horizontal length scales are approximately 0.8 times the orbital excursion at energetic frequency bands. Noisy values were associated with normalizing horizontal coherence with small orbital excursion values. This occurs at high frequencies and frequency bands in which the energy was low because of the combined effects of the decreased spectral density and the ω^{-2} spectral operator. The noisy values above the exponential line fit in Figure 13b are from 28 September. On this day, the peak frequency is in the 0.10 – 0.15

Hz frequency band and the spectral energy in the 0.05 – 0.10 Hz frequency band is small resulting in shorter orbital excursion. Because the orbital excursion is small, scaling the horizontal length scale results in higher values.

The horizontal length scales/orbital excursion likely have a vertical dependence on measurement elevation of the OBS sensors that is not identified in this study. Whereas the horizontal coherence had an approximate exponential decay with distance, the vertical coherence dependence on elevation is not obvious. In some cases, there are distinct layers over which the coherence is uniform (Figure 9a,b), but in others there is a linear or exponential dependence (Figure 11). In some cases the vertical coherence is similar across frequency bands (Figure 9 and 10), but in others there is strong frequency dependence (Figure 11). When the turbidity meters were within a well defined suspended sediment layer, the variability in horizontal coherence is reduced. When the vertical coherence is a linear or exponential decreasing the horizontal coherence variability increases.

B. BEDLOAD LAYER HEIGHT

The observed bedload layer heights are shown in Figure 14 to be approximately twice the theoretical wave boundary layer height (Nielson, 1992)

$$\delta_{.05}/r = 0.26(\xi/2r)^{0.70} \qquad (2)$$

where r is the hydraulic roughness and ξ is the rms orbital amplitude excursion just above the boundary layer calculated using (1) over the frequency band 0 – 1 Hz. The equivalent Nikuradse roughness is $r= 30z_0$. The logarithmic velocity profile over a bed of closely packed spheres of diameter, d, goes through zero at $z_0= 1/30d$ (Nikuradse, 1933).

Therefore, the hydraulic roughness was defined as the diameter of the mean sediment size, 0.2 mm in the absence of local morphology. The top of the boundary layer, $\delta_{.05}$, is defined where the velocity defect amplitude becomes less than 5% of $A\omega$ (Sleath, 1987). The theoretical wave boundary layer ranged from 0.7 – 1.6 cm.

C. VERTICAL COHERENCE

Vertical coherence was observed to be dependent on frequency and cross-shore location. The frequency dependence of the vertical variation of suspended sediment is evident when examining spectra (Figure 8). Near the bed, the concentrations are high and the spectra are broad. The energy at the lowest frequencies is the greatest and the spectral energy decreases slowly with frequency. At heights significantly above the seafloor, the energy in the infragravity band is still significant but at higher frequencies there is a peak in the sediment spectrum similar to the cross-shore velocity spectral peak (Figure 5).

Possible sources of cross-shore dependence of vertical coherence are from bottom morphology, wave height, wave period, water depth, bottom slope and percentage of wave breaking. Dependence of the vertical coherence length scale was investigated with these parameters and all combinations of them, including the surf parameter $(\tan\beta/(H/L_o)^{1/2})$, a saturation parameter (H_{rms}/h) and orbital excursion (ξ). The best correlation that was obtained is the vertical coherence length scale scaled by the depth of water with the orbital excursion scaled by the wave height (Figure 15). The linear correlation coefficient is 0.61, which is significantly different from zero with 95% confidence.

Identifying the mechanisms that relate to the vertical coherence length scale is difficult due to the variety of vertical dependence. In some cases, the vertical coherence is a distinct uniform layer throughout the frequency bands, but in other cases there is a linear or exponential dependence and strong frequency dependence. The difficulty in establishing vertical dependence was similarly found by Sheng and Hay (1995) who were unable to find a scale for the vertical dependence of diffusivity profiles.

V. SUMMARY AND CONCLUSIONS

Suspended sediments were measured using both acoustic and optical backscatter sensors, and associated flow velocities measured with EM current meters. Both acoustic and optical sensors have difficulty distinguishing suspended sediment from the bed from bubbles produced by breaking waves. Thus, this study was restricted to areas with little or no breaking waves occurred.

Acoustic backscatter measurements of suspended sediments by the BCDV every 1.7 cm over the bottom to approximately 65 cm are used to examine the vertical structure of suspended sediments. Bedload layer is differentiated from suspended sediment layer by intercomparing coherence at various levels. The thickness of this decorrelated bedload layer was twice the height of the theoretical wave boundary layer predicted for with no local morphology influences. The vertical coherence length scale of the suspended sediment layer is determined to be an order of magnitude greater than the bedload layer and to be dependent on orbital excursion, wave height, and water depth. At the deepest locations, where the bottom is smooth and orbital excursion and H_{rms}/h are small, a distinct suspended sediment layer was present. In shallower water, with larger orbital excursion and H_{rms}/h values, differences between suspended sediment frequency bands increased and the distinctive height delineation of the suspended sediment layer is not as well defined. Infragravity wave driven suspended load reached highest elevations above the bed, with higher frequencies having shorter vertical extent. This is attributed to the depth of water acting as a low pass filter on the wave energy disturbing the sediments.

The horizontal length scale was calculated from the coherence between six OBS sensors measurements in a 2 m lagged array at an elevation of approximately 18 cm above the bed. The horizontal coherence length scale is defined as the e-folding scale of the exponentially decreasing coherence with cross-shore distance. The horizontal suspended sediment length scales were found to be frequency, wave height and orbital excursion dependent. As frequency increased, the horizontal length scale decreased, with the greatest horizontal suspended sediment length scales in the infragravity wave band and peak frequency band of the wave energy. This dependence was removed by scaling the horizontal coherence length by the orbital excursion, which includes the effects of energy and frequency. It is likely there is a vertical dependence of the horizontal length scale that we were not able to determine from these data. The horizontal length scale was found to be 0.8 times the orbital excursion for the frequency range of 0.0 – 0.15 Hz.

Orbital excursion and horizontal suspended sediment length scales compared well out to 0.15 Hz. Above 0.15 Hz, the orbital excursion is so small that using it to normalize the horizontal length scale does not give reliable results. Small orbital excursion at higher frequencies occurs because of the combined effects of the decreased spectral density and the ω^{-2} spectral operator.

The cross-shore dependence of the vertical coherence scale was with bottom slope, wave height, wave length, and depth of water and orbital excursion. The best linear correlation relationship was vertical coherence length scale scaled by the depth of water with the orbital excursion scaled by the wave height. The linear correlation coefficient was 0.61, which is statistically significant with 95% confidence.

LIST OF REFERENCES

Bagnold, R. A., The flow of cohesionless grains in fluids, *Phil Trans Roy Soc Lond*, No 964, Vol 249, 235-297, 1956.

Beach, R. A. and R. W. Sternberg, Suspended sediment transport in the surf zone: response to breaking waves, *Cont. Shelf Res.*, 16(15), 1989-2003, 1996.

Beach, R. A. and R. W. Sternberg, The influence of infragravity motions on suspended sediment transport in the inner surf zone of a highly dissipative beach, *Coastal Sediments '87*, 913 – 928, American Society of Civil Engineers, New York, 1987.

Gallagher, E. L., W. Boyd, S. Elgar, R. T. Guza, and B. Woodward, Performance of a sonar altimeter in the nearshore, *Marine Geology*, 133, 241-248, 1996.

Hanes, D. M., Suspension of Sand Due to Wave Groups, *J. Geophys. Res.*, 96, 8911-8915, 1991.

Hay, A. E. and A. J. Bowen, Coherence scales of wave induced suspended sand concentration fluctuations, *J. Geophys. Res.*, 99, 12749-12765, 1994.

Nielson, P., Coastal Bottom Boundary Layers and Sediment Transport, edited by P. L-F Liu, World Scientific Publishing Co. Pte. Ltd., Singapore, 1992.

Nikuradse, J., Stromungsgesetze in glatten und rauhen rohren, *V D I Forschungsheft*, 361, Berlin, 1933.

Sheng, J. and A. E. Hay, Sediment eddy diffusivities in the nearshore zone, from multifrequency acoustic backscatter, *Cont. Shelf Res.*, 15(2/3), 129-147, 1995.

Sleath, J. F. A., Turbulent oscillatory flow over rough beds, *J. Fluid Mech*, 182, 369-409, 1987.

Stanton, T. P. and K. M. Kohanowich, Calibration of a Coherent Acoustic Sediment Profiler (CASP) and Analysis of Sediment Transport During Duck94, paper submitted to Coastal Engineering, 1998.

Yu, Y. and R. W. Sternberg and R. A. Beach, Kinematics of breaking waves and associated suspended sediment in nearshore zone, *Cont. Shelf Res.*, 13(11), 1219-1242, 1993.

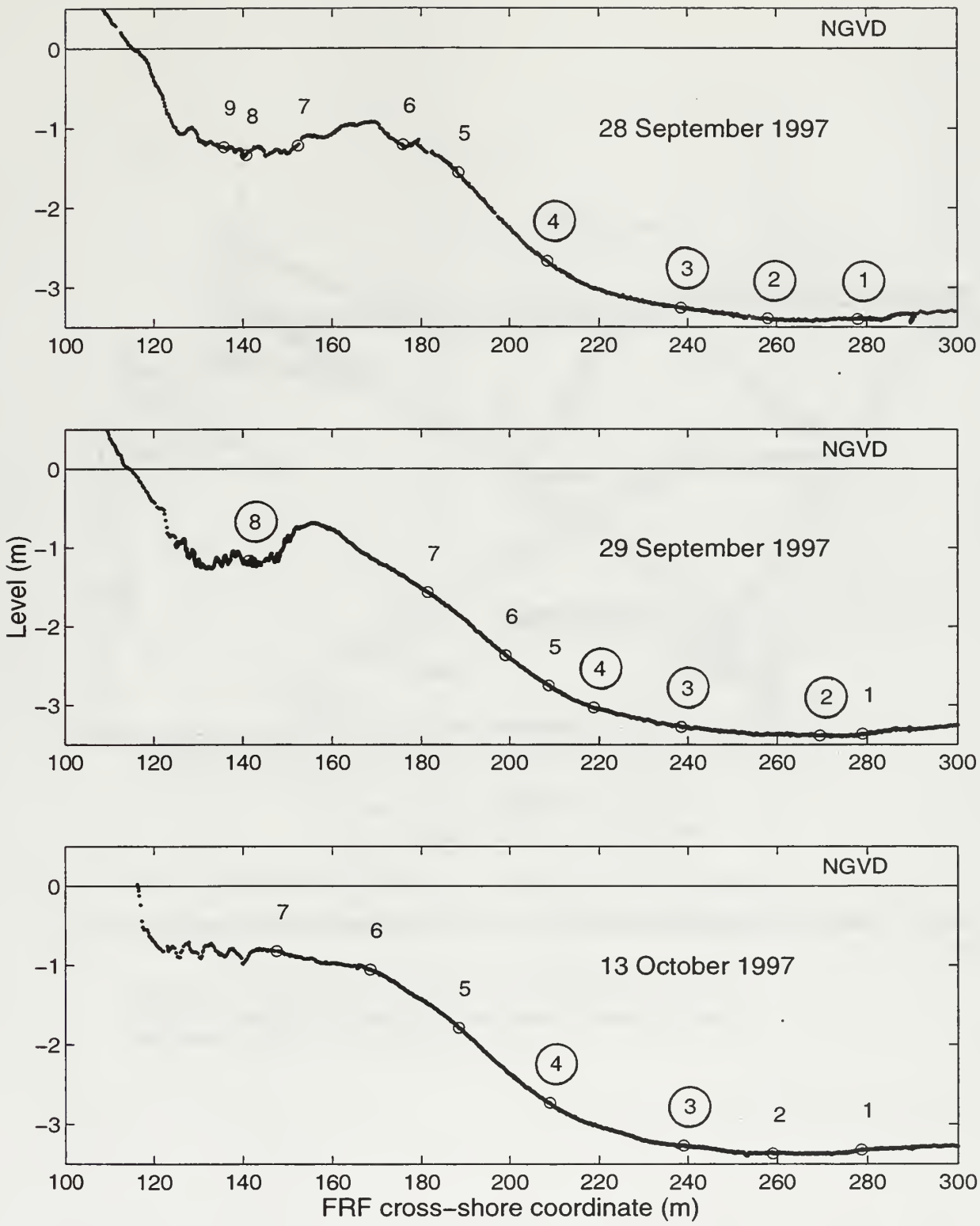

Figure 1. Depth of water and station location for all three days of interest. The depth of water at FRF line 9 as measured by the CRAB and the seven altimeters attached to the CRAB. Measurements were taken on this line at approximately 0700 each morning. The circled stations are the stations to be examined in detail.

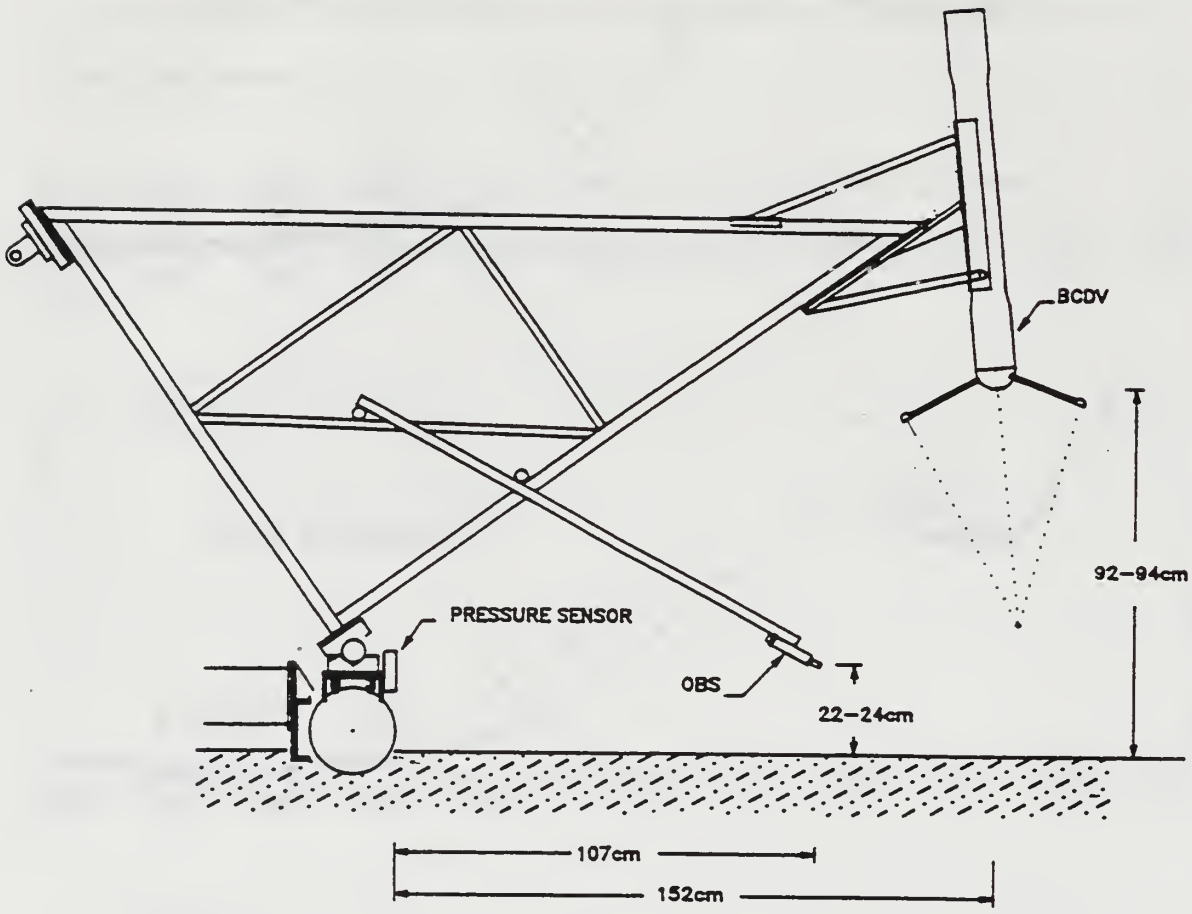

Figure 2. Schematic Drawing of movable cantilever arm and representation of sensors attached to the arm.

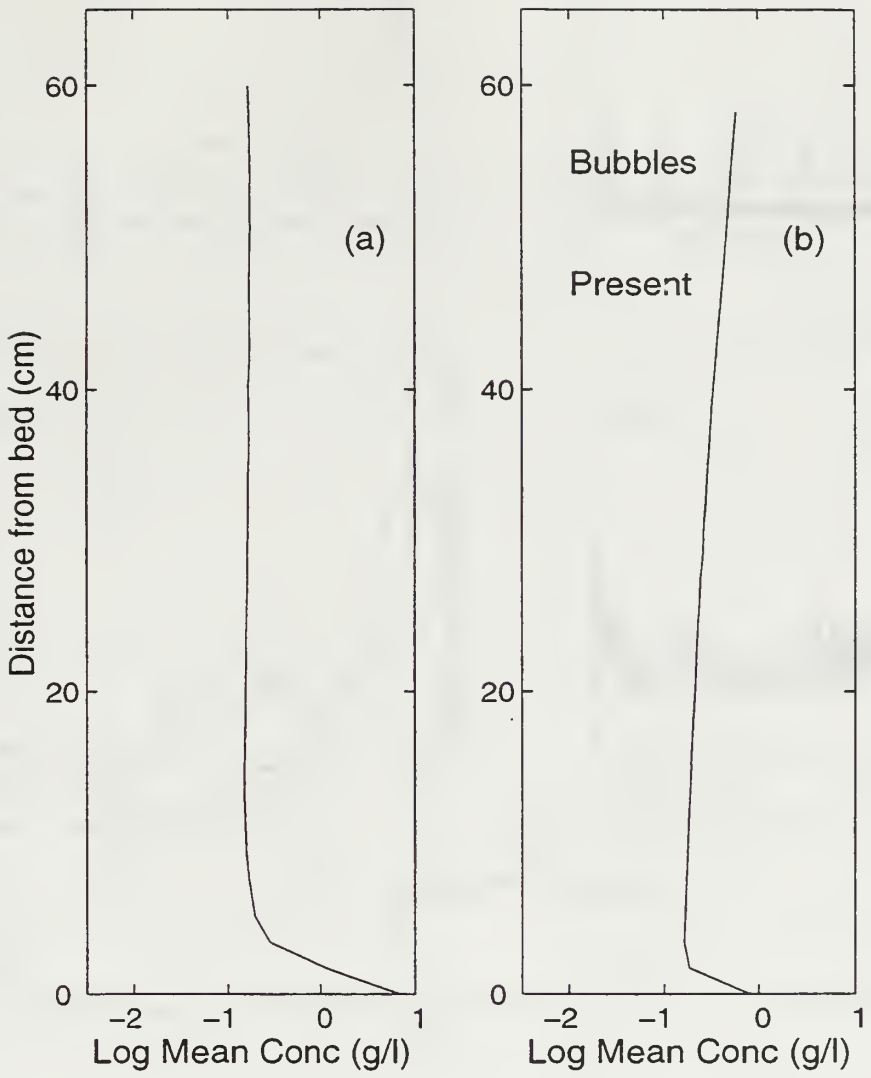

Figure 3. a) Log Mean Concentration for 28 September at station 4. No obvious bubbles are present. b) Log Mean Concentration for 28 September at station 7. Bubbles are present.

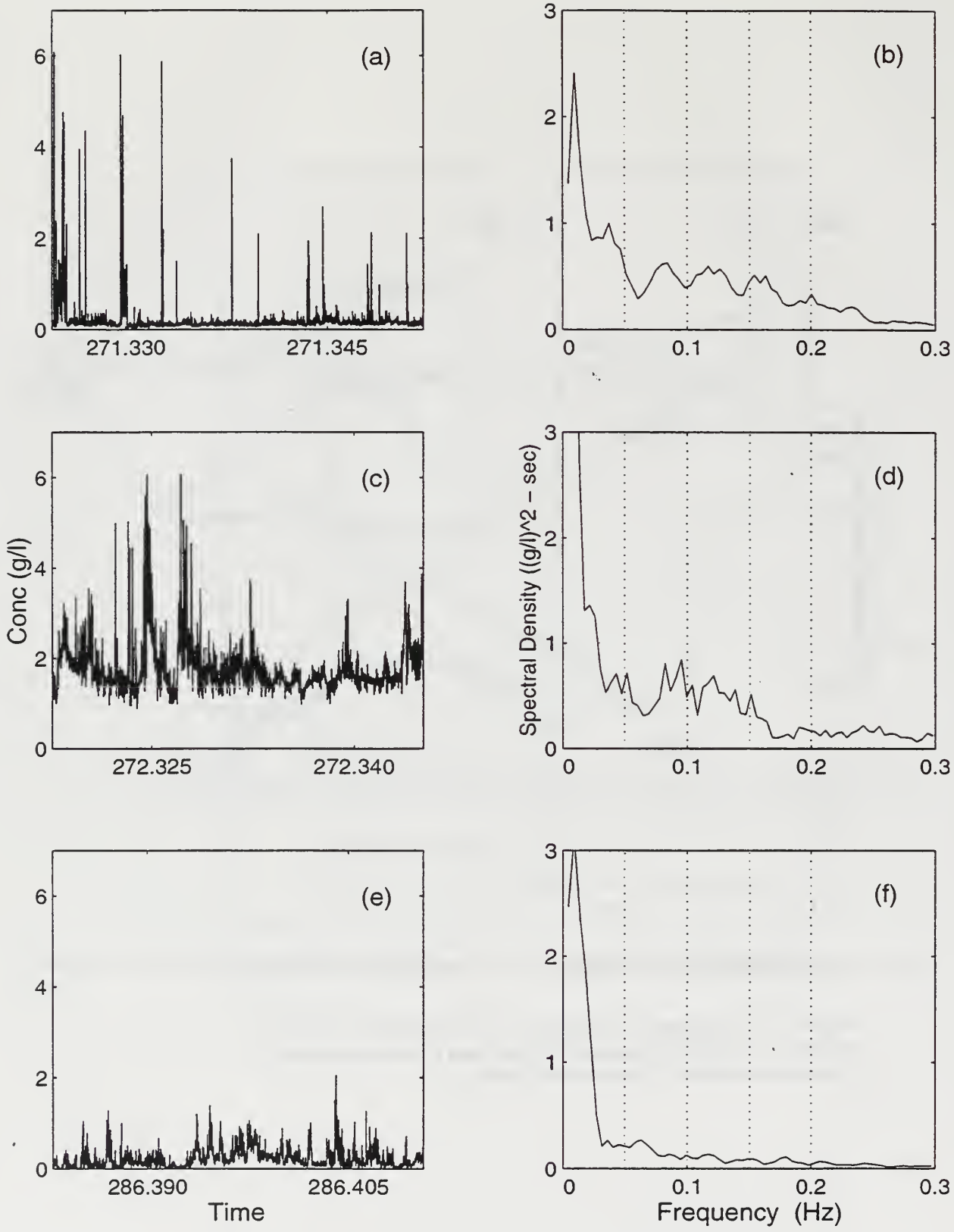

Figure 4. Forty minute portion of time series of suspended sediment concentration and corresponding spectral density for entire one hour period on station. a) Time series for station 2 on 28 September. b) Spectral density for station 2 on 28 September. c) Time series for station 2 on 29 September. d) Spectral density for station 2 on 29 September. e) Time series for station 3 on 13 October. f) Spectral density for station 3 on 13 October.

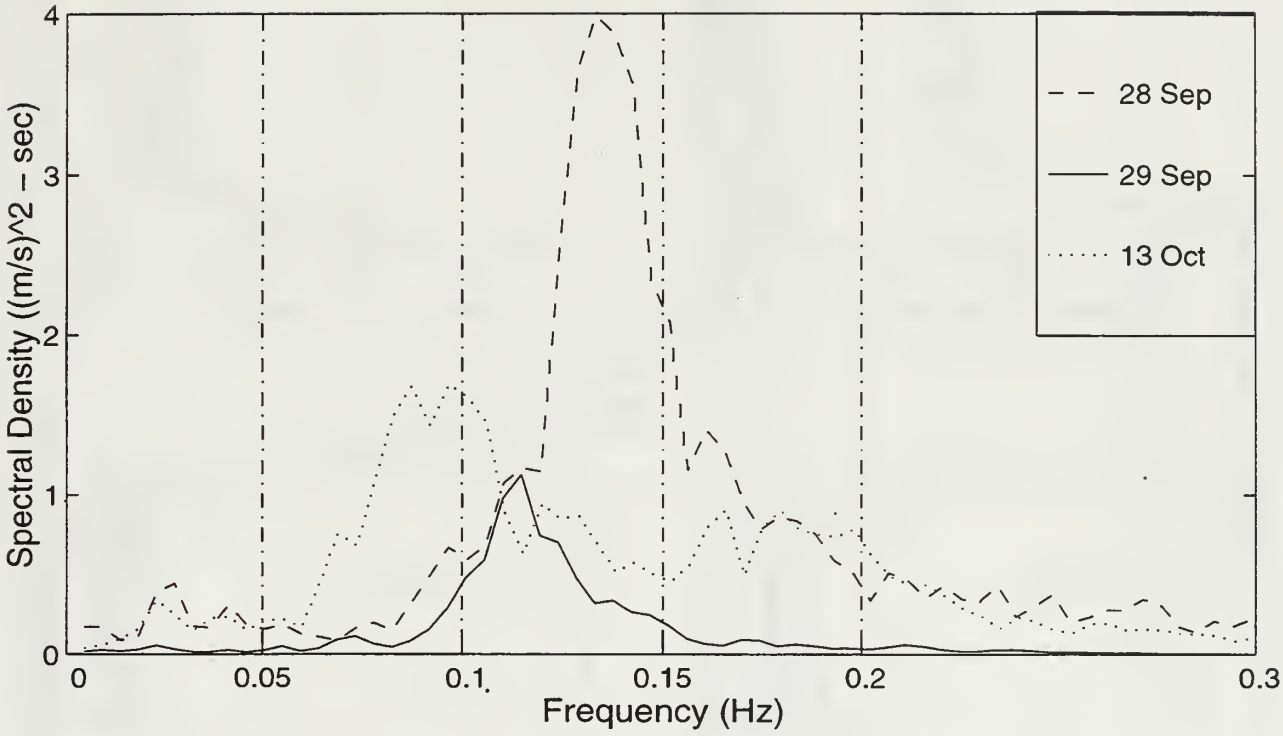

Figure 5. Spectral density of cross-shore current at station 4 for three days investigated.

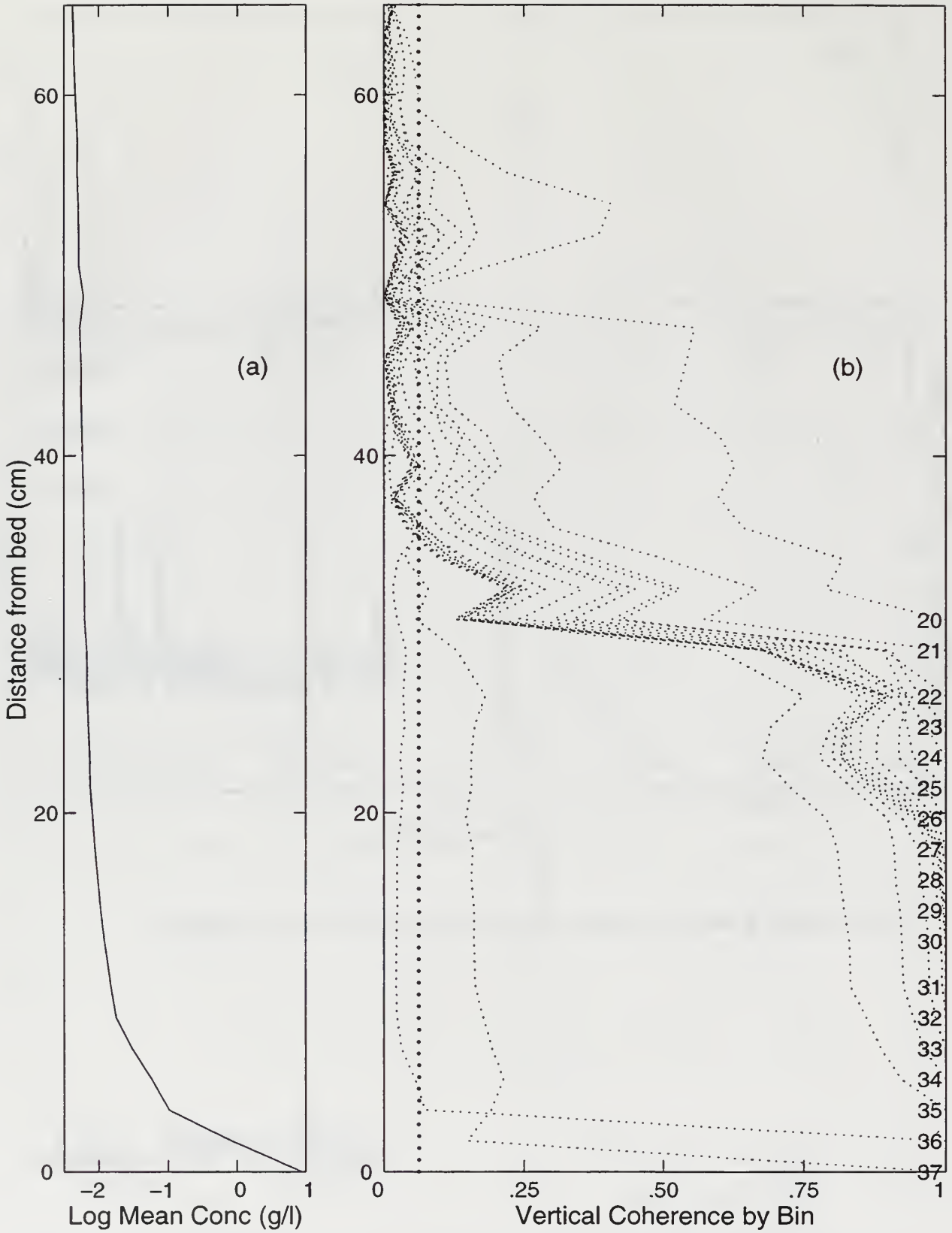

Figure 6. a) Log Mean Concentration for 28 September at station 1. b) The coherency between adjacent bins averaged over the 0.1 – 0.15 Hz frequency band. The vertical dotted line indicates the coherence level significantly different from zero at the 95% confidence interval.

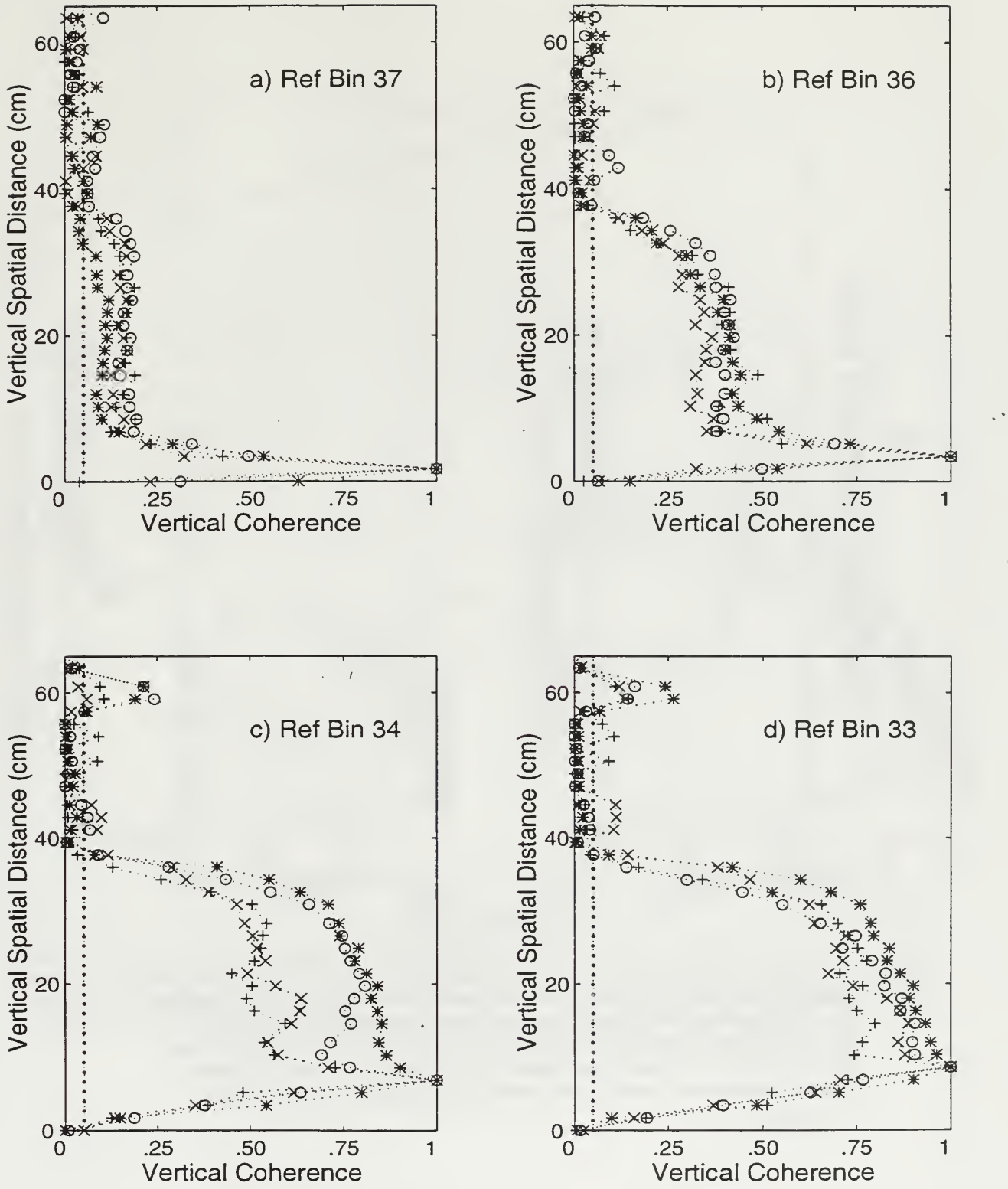

Figure 7. a) The vertical coherence for 28 September at station 2 using bin 37 as the reference bin. b) The vertical coherence for 28 September at station 2 using bin 36 as the reference bin. c) The vertical coherence for 28 September at station 2 using bin 34 as the reference bin. d) The vertical coherence for 28 September at station 2 using bin 33 as the reference bin. The vertical dotted line indicates the coherence level significantly different from zero at the 95% confidence interval. * 0.0 – 0.05 Hz, o 0.05 – 0.10 Hz, x 0.10 – 0.15 Hz, + 0.15 –0.20 Hz.

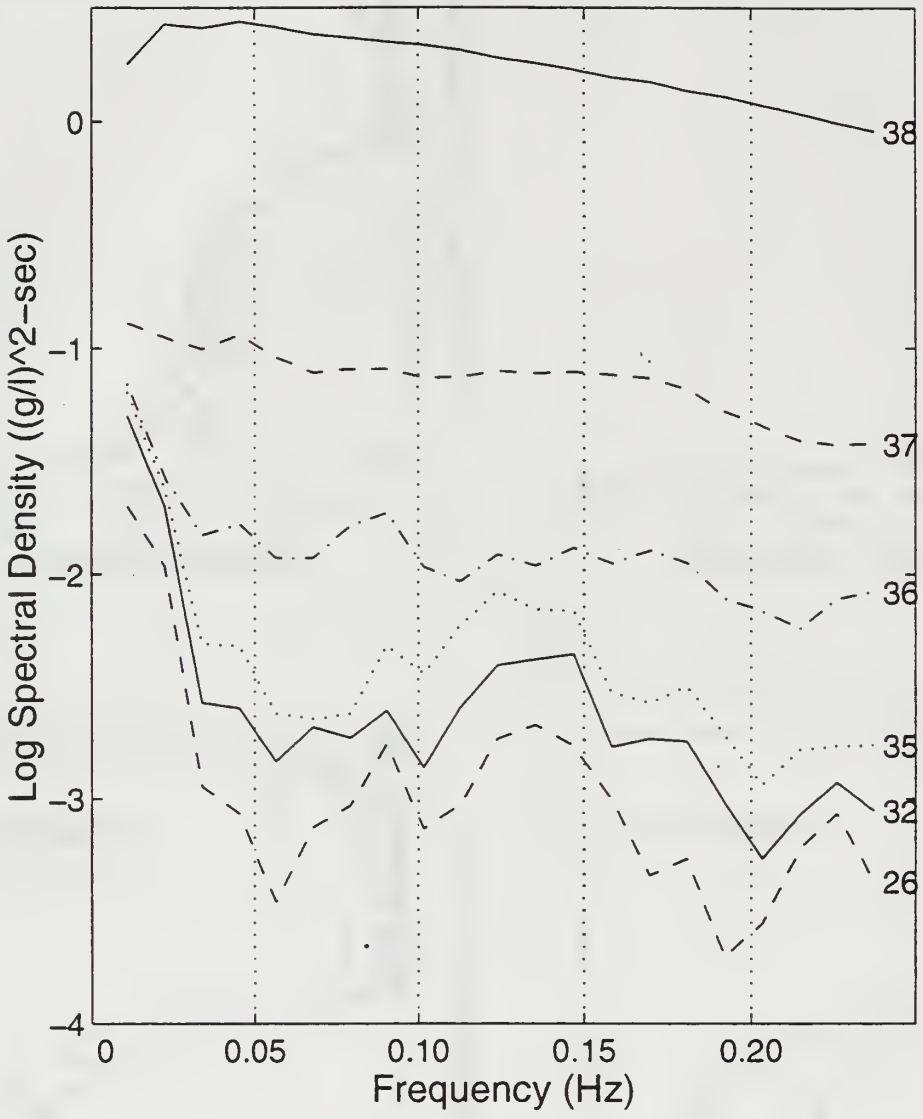

Figure 8. Log of the spectral density of suspended sediments at discrete bins for 29 September at station 4. The bin numbers are on one side of the spectrum. The seabed is bin 38, the wave boundary layer is below bin 36 (elevation 3.4 cm) and the reference bin is bin 35 (elevation 5.1 cm). Bin 26 is at an elevation of 20.4 cm. The dashed vertical lines delineate the frequency bands that were investigated.

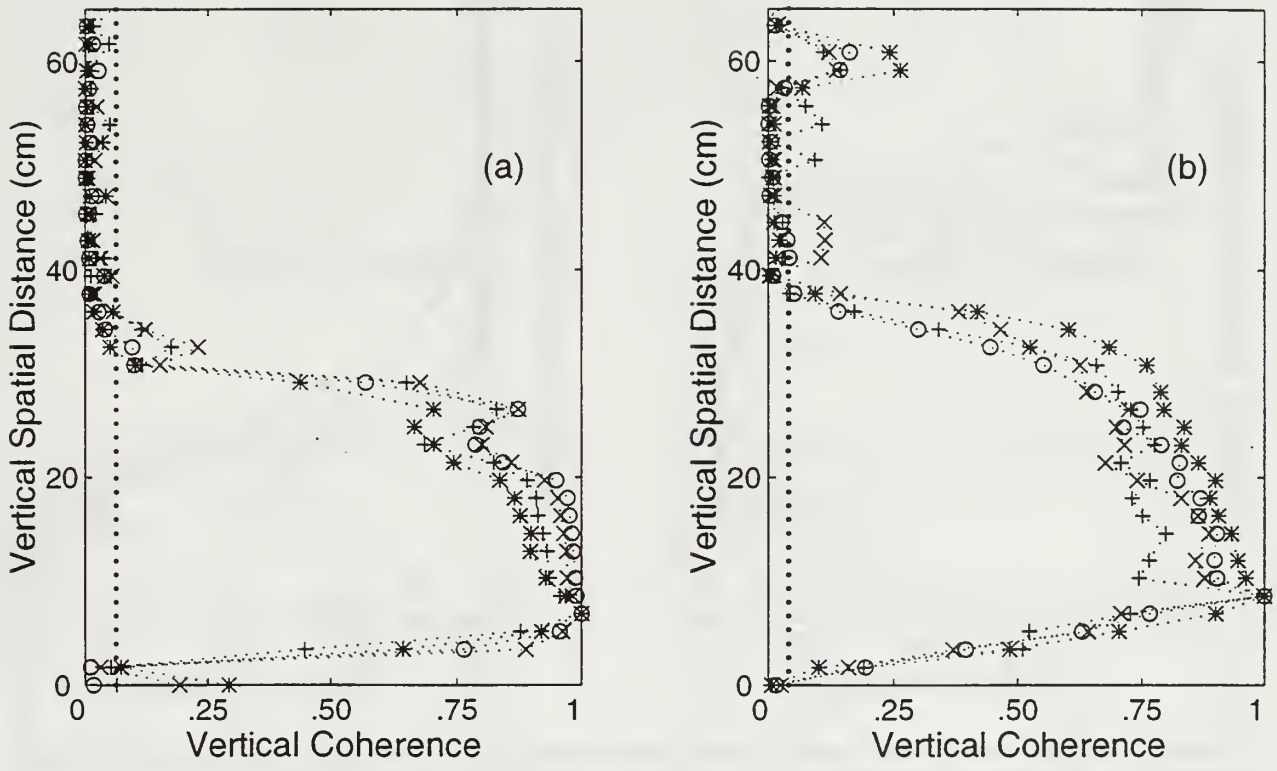

Figure 9. a) The vertical coherence for 28 September at station 1. The reference bin is 6.9 cm above the seafloor. b) The vertical coherence for 29 September at station 2. The reference bin is 8.6 cm above the seafloor. The vertical dotted line indicates the coherence level significantly different from zero at the 95% confidence interval. * 0.0 – 0.05 Hz, o 0.05 – 0.10 Hz, x 0.10 – 0.15 Hz, + 0.15 –0.20 Hz.

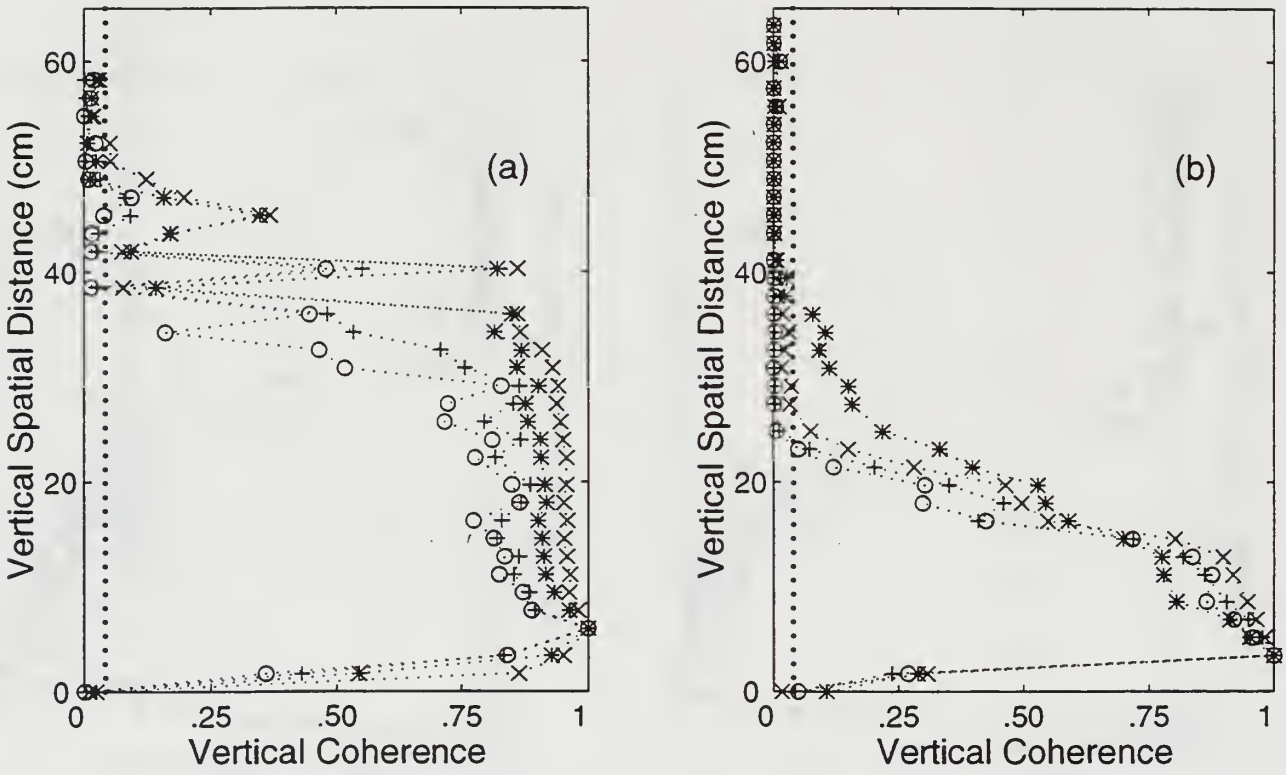

Figure 10. a) The vertical coherence for 29 September at station 3. The reference bin is 6.0 cm above the seafloor. b) The vertical coherence for 28 September at station 2. The reference bin is 3.4 cm above the seafloor. The vertical dotted line indicates the coherence level significantly different from zero at the 95% confidence interval. * 0.0 – 0.05 Hz, o 0.05 – 0.10 Hz, x 0.10 – 0.15 Hz, + 0.15 –0.20 Hz.

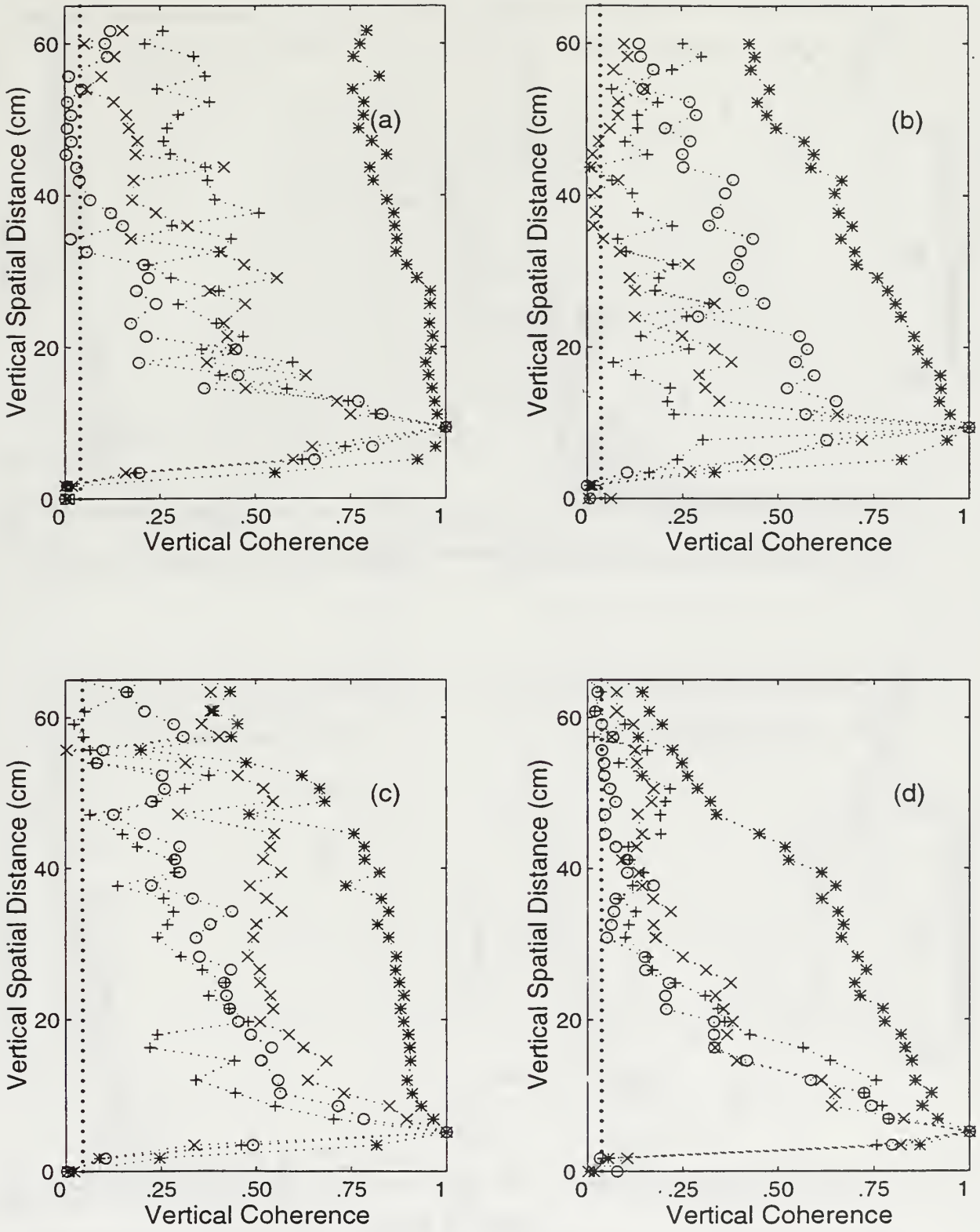

Figure 11. a) The vertical coherence for 28 September at station 3. The reference bin is 9.4 cm above the seafloor. b) The vertical coherence for 28 September at station 4. The reference bin is 9.4 cm above the seafloor. c) The vertical coherence for 29 September at station 4. The reference bin is 5.1 cm above the seafloor. d) The vertical coherence for 13 October at station 3. The reference bin is 5.1 cm above the seafloor. The vertical dotted line indicates the coherence level significantly different from zero at the 95% confidence interval. * 0.0 – 0.05 Hz, o 0.05 – 0.10 Hz, x 0.10 – 0.15 Hz, + 0.15 –0.20 Hz.

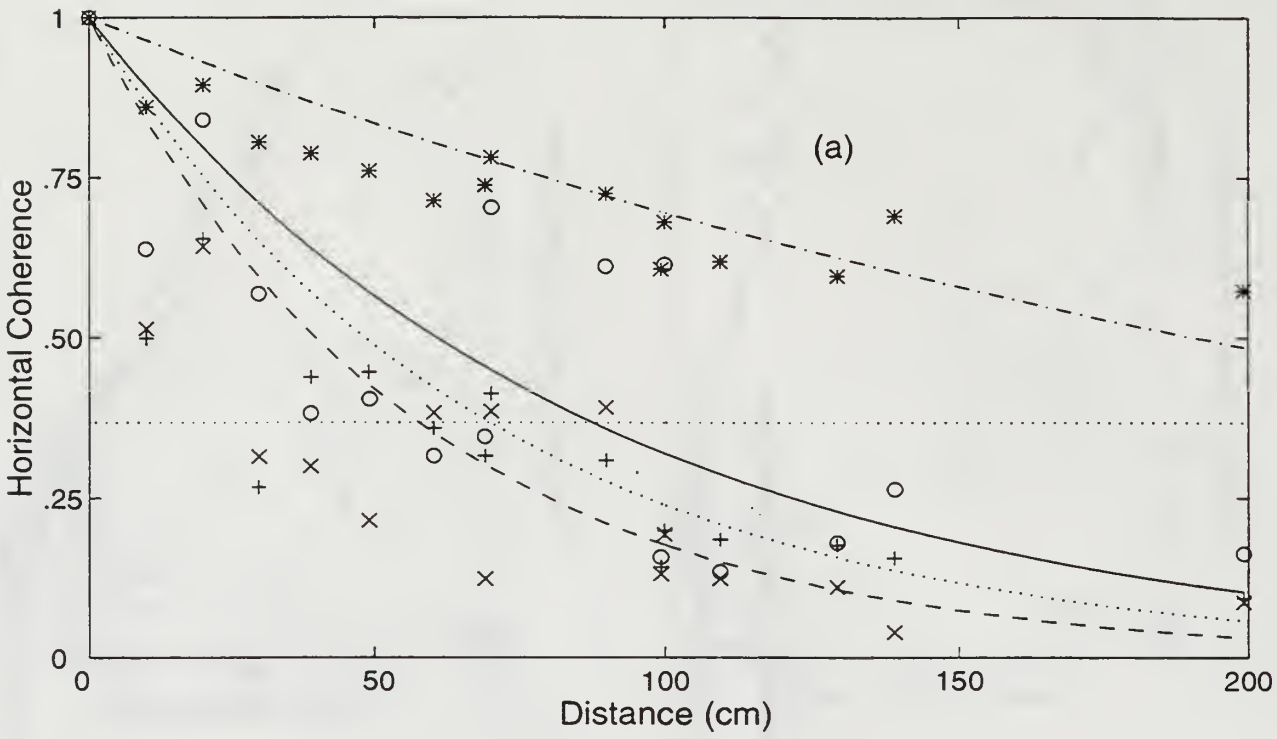

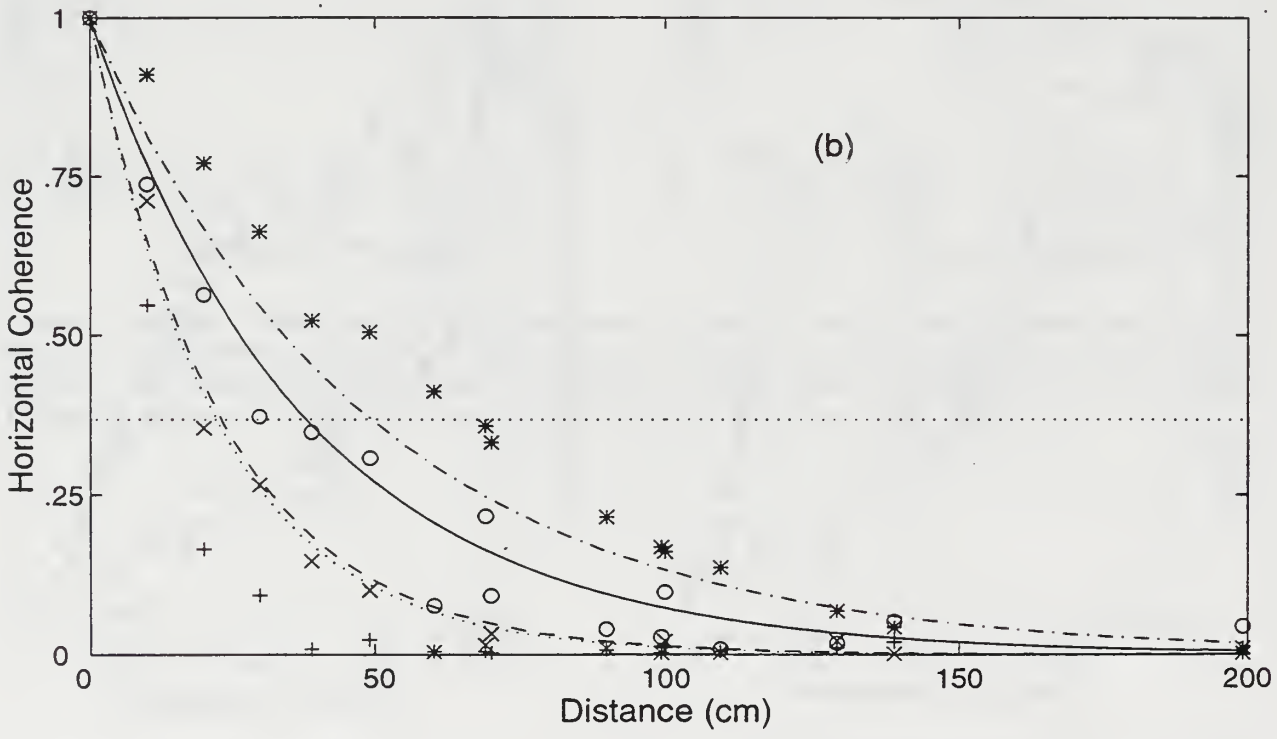

Figure 12. a) The horizontal coherence for 28 September at station 4. b) The horizontal coherence for 29 September at station 4. The data are compared with least square exponential curve. The horizontal coherence length is defined by exponential curve intersecting the e-folding scale (dotted horizontal line). (- . - . *) 0.0 – 0.05 Hz, (- - x) 0.05 – 0.10 Hz, (— o) 0.10 – 0.15 Hz, and (. . . +) 0.15 –0.20 Hz.

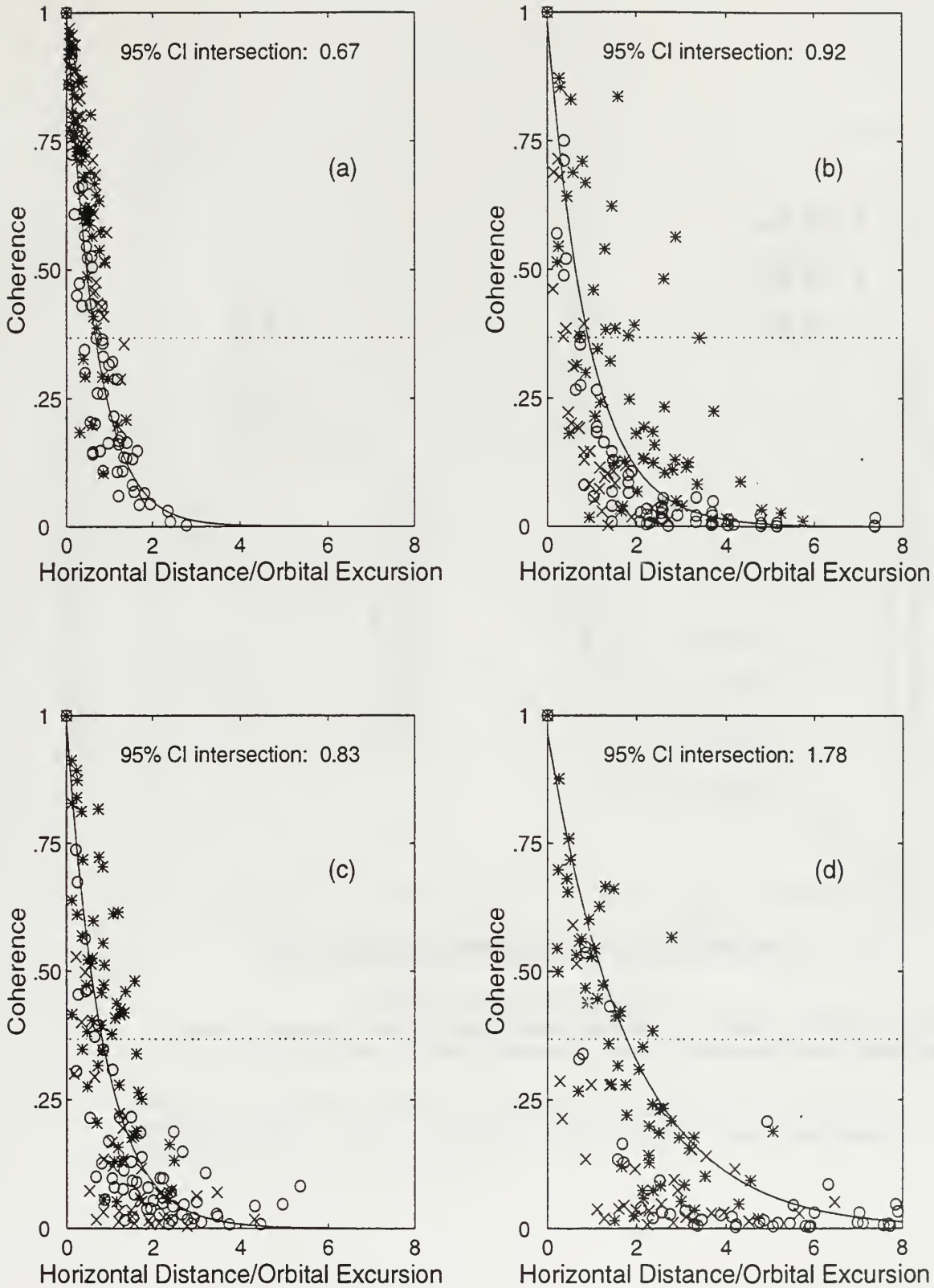

Figure 13. Horizontal coherence parameterized by orbital excursion for all three days and stations investigated. a) 0.0 – 0.05 Hz b) 0.05 – 0.10 Hz c) 0.10 – 0.15 Hz d) 0.15 – 0.20 Hz. * 28 September, o 29 September, x 13 October

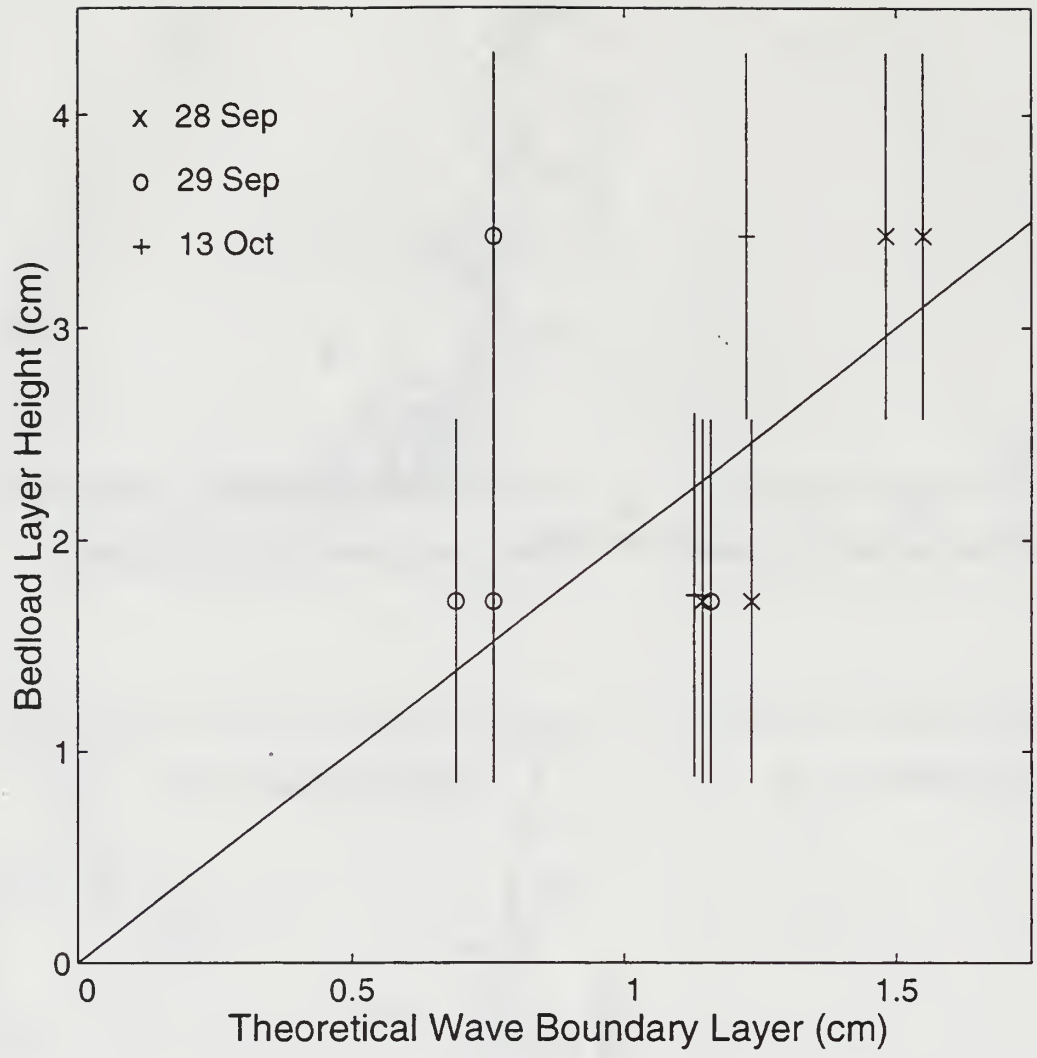

Figure 14. The theoretical wave boundary layer plotted against the measured bedload layer height. Error lines are due to the uncertainity of the discrete bin size.

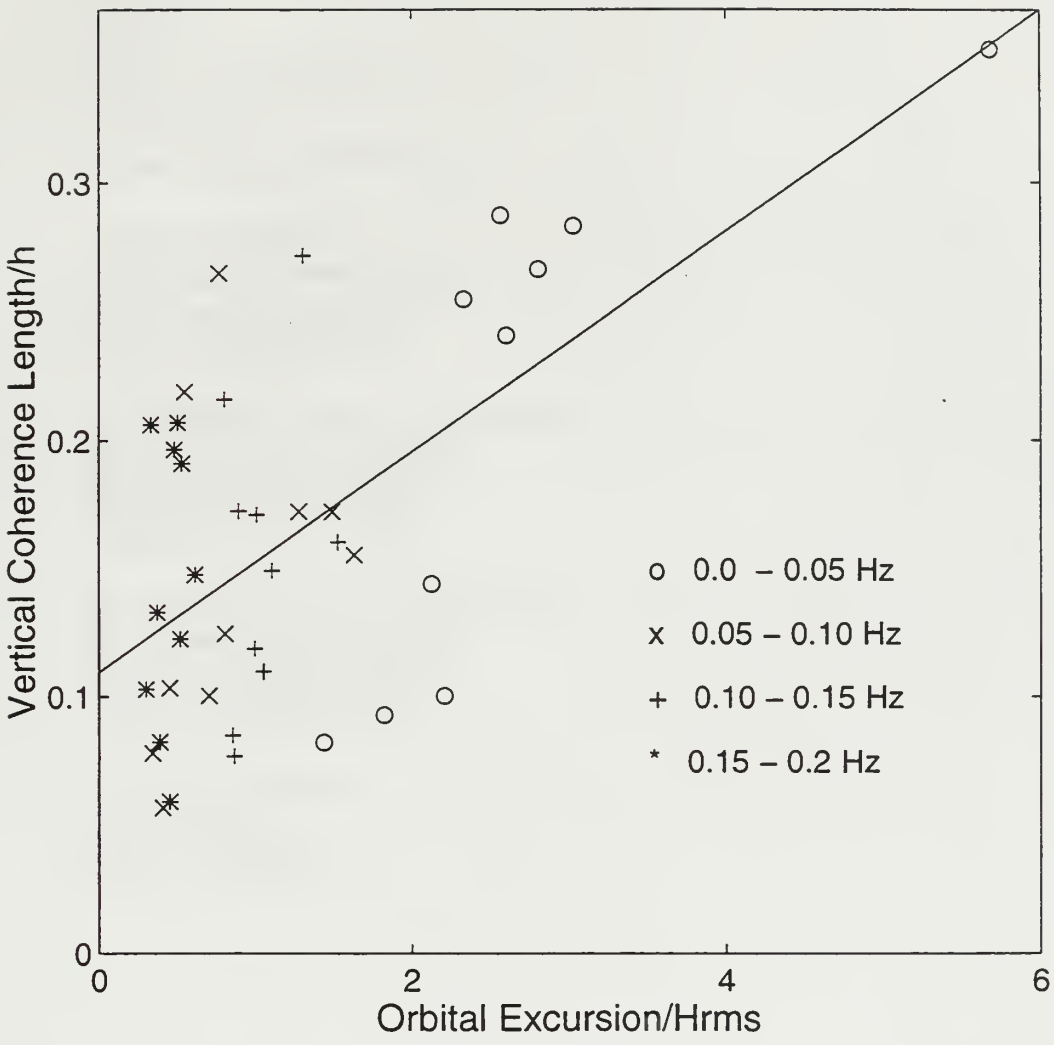

Figure 15. Vertical length scale over depth of water in relation to orbital excursion over the wave height. The linear correlation coefficient is 0.61 which is significantly different from zero with 95% confidence.

INITIAL DISTRIBUTION LIST

No. Copies

1. Defense Technical Information Center.....2
   8725 John J. Kingman Rd, STE 0944
   Ft. Belvoir, VA 22060-6218

2. Dudley Knox Library.....2
   Naval Postgraduate School
   411 Dyer Rd
   Monterey, CA 93943-5101

3. Chairman (Code OC/Bf)... 1
   Department of Oceanography
   Naval Postgraduate School
   Monterey, CA 93943-5122

4. Dr. Edward B. Thornton (Code OC/Th).....4
   Department of Oceanography
   Naval Postgraduate School
   Monterey, CA 93943-5122

5. Dr. Timothy P. Stanton (Code OC/St).....2
   Department of Oceanography
   Naval Postgraduate School
   Monterey, CA 93943-5122

6. LT Michael P. Huck.....2
   3104 Coffey Ave
   Bellevue, NE 68123